Review

Piezoelectric Actuators – Recent Innovations 2024 –

Kenji Uchino *

Posted Date: 30 January 2024

doi: 10.20944/preprints202401.2073.v1

Keywords: Piezoelectric actuators; High-power density piezoelectrics; Multilayer actuators; MEMS; PZT; PMN; Politico-engineering; Crisis technology; Sustainability technology; Piezoelectric energy harvesting; DC/DC converter

Review

Piezoelectric Actuators—Recent Innovations 2024

Kenji Uchino [1,2]

[1] Emeritus Academy Institute, The Pennsylvania State University, University Park, PA 16802, USA; kenjiuchino@psu.edu

[2] Board Member (Secretary), Micromechanics Inc., State College, PA 16802, USA

Abstract: This article reviews recent innovations in piezoelectric actuators, then indicates the future research targets. In the materials, the piezoelectric performances of relaxor-lead titanate (PZN-PT, PMN-PT) single crystals have been improved significantly by an AC electric poling technique. Also new loss characterization techniques facilitate developing high-power density piezoelectrics. The RMS vibration velocity reaches 0.6 m/s in the k_{31} mode in lead zirconate titanate (PZT) nowadays, which corresponds to power density 30 W/cm^3. Pb-free materials are urged due to the recent political regulation on toxic materials. In device designs, the original multilayer actuators (MLA) with Ag/Pd electrode have been switched to the ones with Cu or pure Ag, in order to suppress the heat generation, then to enhance the device power density. Piezoelectric micro-electro-mechanical-systems (MEMS's) started to utilize the <1 0 0> oriented epitaxial films of rhombohedral PZT compositions, which exhibits enhanced piezoelectric properties. Also for higher-power applications, aero-sol deposition (AD) methods have been introduced to 10 μm-thick films. Regarding drive/control techniques in piezo-actuators, three developments are on-going, that is, "negative capacitance" power supplies for driving off-resonance (pseudo-DC) piezo-actuators, capacitive AC power supplies for efficiently driving resonance piezo-actuators, and DC/DC converters for harvesting electric energy from high-impedance piezoelectric devices under noise vibration. The applications of piezoelectric actuators in the 21st century seem to be oriented toward "politico-engineering" with four keywords, "cooperation, protection, reduction, and continuation". The sustainability technologies include the following piezoelectric items: (a) Pb-free piezoelectrics, (b) ultrasonic technology for decomposing hazardous materials, (c) reduction of contamination gas, (d) piezoelectric energy harvesting, and (e) device improvement with high energy-efficiency. On the other hand, the following crisis technologies have been developed with piezoelectrics: (a) detection and neutralization technologies of infectious/epidemic diseases such as anthrax, (b) autonomous unmanned underwater, aerial, and land vehicles with piezoelectric actuators, (c) pin-point target weapons, (d) high voltage supplies with piezoelectric transformers, and (e) compact energy sources for remote actuating/sensing systems.

Keywords: piezoelectric actuators; high-power density piezoelectrics; multilayer actuators; MEMS; PZT; PMN; politico-engineering; crisis technology; sustainability technology; piezoelectric energy harvesting; DC/DC converter

1. Historical Background

"Piezoelectric actuators", named by Uchino in the early 1980s in his book [1], have been commercialized in cameras, office equipment and automobiles in the end of 20th century, in accordance with the Japanese governmental slogan, "lighter, thinner, shorter, and smaller (軽薄短小 in a 4-Chinese-Character word)". The readers can refer to the textbooks [2-8] on the historical background of piezoelectric actuators. However, their industrial developments were decelerated after the worldwide economic recession in the 1990s. Since the 21st century started from the terrorist attack on World Trade Center in the US, Uchino proposed the new industrial development slogan toward "politico-engineering" (i.e., politically-initiated engineering) with four keywords, "cooperation, protection, reduction, and continuation (協守減維)" [5]. Worldwide cooperation on emission regulation of environmental gases such as CO_2, NO_x, SO_x accelerates new technologies. Self-protection of a country against the terrorists or territorial aggressors is the must by developing pin-point-target weapons. On the other hand, we need to promote reduction of toxic materials and

 doi:10.20944/preprints202401.2073.v1

electricity usage. Then continuation of human life and society urges the sustainability engineering, including medical technologies, food engineering, renewable energy harvesting.

This paper reviews recent innovations in piezoelectric actuators. We will discuss the following items in separate chapters: (1) Piezoelectric materials improvement, from both "real" part (electromechanical coupling) and "imaginary" part (loss) viewpoints. (2) Actuator device designs, Cu-electrode multilayers and thick film MEMS's. (3) Drive/control techniques to increase the power efficiency, and (4) various crisis and sustainability applications toward "politico-engineering" with four keywords, "cooperation, protection, reduction, and continuation".

2. Performance Improvement of Piezoelectric Materials

After the discovery of huge piezoelectric performances in $PbZrO_3$-$PbTiO_3$ (PZT) ceramics in the middle of 1950s [9,10], these PZT compositions have been the majestic industrial materials up to now for 70 years. On the contrary, a research fever on actuator applications was ignited in 1979 by the discovery of giant electrostriction in $Pb(Mg_{1/3}Nb_{2/3})O_3$-$PbTiO_3$ (PMN-PT) ceramics [11-14]. Though the non-hysteretic PMN-based electrostrictive actuators have successfully been utilized in a Hubble telescope on the Space Shuttle by NASA [15], their large capacitance of the electrostrictive multilayers limited the high-speed applications with wide commercialization.

In parallel, superior piezoelectric performance was discovered in single crystals of $Pb(Zn_{1/3}Nb_{2/3})O_3$-$PbTiO_3$ (PZN-PT) [16,17] in 1981. The key to the performance improvement is the crystal orientation: Electric field was applied along the perovskite <0 0 1> axis on a rhombohedral PZN-PT crystal with the spontaneous polarization along the <1 1 1> axis. The large effective piezoelectric constant d_{33}^{eff} was explained by large shear d_{15} contribution generally observed in perovskite piezo-ceramics, as visualized in Figure 1. When the electric field E is parallel to the spontaneous polarization P_S direction in the tetragonal crystal, the oxygen octahedron should be elongated [Figure 1a]; while the electric field E along <0 0 1> cants from the P_S along <1 1 1> by 71° in the rhombohedral composition, the oxygen octahedron rotates without significant distortion, corresponding to the d_{15} mode. Thus, due to this shear contribution, the effective piezoelectric constant d_{33}^{eff} is apparently enhanced [17-20]. The initial large investment in the 1990s from the US Navy was for developing innovative submarine sonar systems sensitive particularly to low frequency lower than 20 kHz in the 21st century.

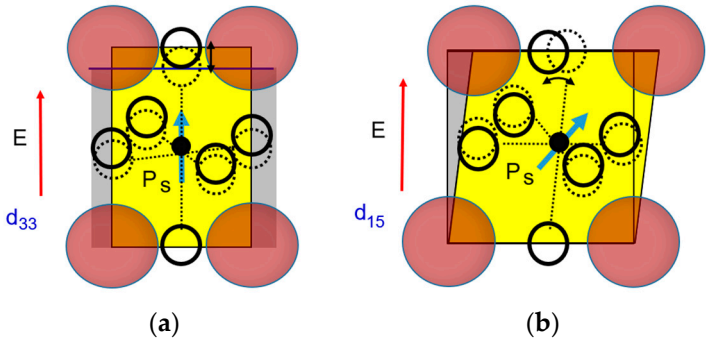

Figure 1. Visualization of the enhancement of the effective piezoelectric constant d_{33}^{eff}. (a) Electric field E parallel to the spontaneous polarization P_S in a tetragonal phase; (b) E is not parallel to P_S in a rhombohedral phase. Since the oxygen octahedron can easily rotate via the shear deformation d_{15} contribution, the d_{33}^{eff} is enhanced.

2.1. Relaxor Single Crystals

The recent researchers seem to use the AC poling (ACP) specimen preparation technique (invented by Yamamoto et al. [21]) to enhance piezoelectric properties for $Pb(Mg_{1/3}Nb_{2/3})O_3$-$PbTiO_3$ (PMN-PT) in comparison with conventional DC poling (DCP) [22–24]. Qiu et al. [24] reported two items on the performance improvement: first, the d_{33}^{eff} for perovskite [0 0 1]-oriented rhombohedral PMN–0.28PT single crystals became higher with increasing the thickness of the plate specimen from

100, 200, and 500 μm. Second, the ACP treatment provided d_{33}^{eff} improvement more than 20% than the DCP specimens. In parallel, Sun et al. demonstrated the piezoelectric coefficient as high as d_{33}^{eff} > 1950 pC/N in PMN–0.28PT single crystals by low-voltage ACP of 1.5–3.5 kV_{rms}/cm at an elevated temperature of 80℃ in an air atmosphere [22]. Their ACP preparation method improved also the standard deviation of permittivity ε_{33}^{X}, comparable to that of the conventional DCP. For example, $\varepsilon_{33}^{X}/\varepsilon_0 = 8800 \pm 170$ under a 2.0 kV_{rms}/cm of ACP satisfies the required quality for the medical acoustic probes.

The ferroelectric domains on 71°-sided walls merge effectively under the ACP, leading to a considerable increase in the domain size, thus, a significant enhancement of electromechanical properties. Qiu et al. [24] also conducted a computer simulation for the domain size increase to create lamellar configurations during the ACP process, which deduces the higher dielectric permittivity and effective piezoelectric constants.

[CURRENT ISSUE] Though the dielectric loss was not increased through the ACP process, the author is anticipating the mechanical quality factor (i.e., elastic loss) degradation with the vibration velocity for this "softening" process (i.e., higher permittivity and piezoelectric constant), which blocks high-power piezoelectric applications. Clarification is desired urgently on this possible problem.

2.2. High-Power Density Piezoelectrics

The evaluation criterion of the piezoelectrics seems to be gradually shifting from the "real" part to "imaginary" part performances in the 21st century; that is, piezoelectric loss, elastic loss $s^{E''}$ rather than piesoelectric constant d, elastic compliance $s^{E'}$ [7]. Piezoelectric devices operated at the resonance frequency such as ultrasonic motors and piezoelectric transformers induce siginificant heat with increasing the vibration level above a critical vibration velocity. We define the "maximum vibration velocity v_{max}" under which temperature rise of 20°C from room temperature is observed. Most of the currently commercialized PZT piezoceramics exhibit the $v_{max}^{rms} = 0.3m/s$ in the k_{31} plate mode, which corresponds to the power density around 7 W/cm³.

2.2.1. High-power density piezoelectrics commercialized

NEC Corporation developed the PZT-Pb($Mn_{1/3}Sb_{2/3}$)O_3 (PMS-PZT) ceramics with the $v_{max}^{rms} = 0.62m/s$ in 1996, which could be widely commercialized as piezo-transformers for the laptop LCD backlight converters [25]. By doping the PMS-PZT or Pb(Mn,Nb)O_3-PZT with rare-earth ions such as Yb, Eu and Ce, Uchino's group further improved high power performance, operational with v_{max}^{rms} up to 1.0 m/sec in the early 2000s [26,27]. Compared with commercially available piezoelectrics, 10 times higher input electrical and output mechanical energy (evaluated by square of v_{max}^{rms}) can be expected from these new materials without generating significant temperature rise, which corresponds to 50 W/cm³.

[CURRENT ISSUE] Though the current PZT-based products with $v_{max}^{rms} = 0.62m/s$ and power density 30 W/cm³ are not bad, wider commercialization of piezo-ceramics with $v_{max}^{rms} = 1\ m/s$ and 50 W/cm³ will be the ultimate industrical desire in the 21st century. As introduced in Section 2.3, Pb-free piezoelectrics will be an alternative material category. Dopant optimization in (Na,K)NbO_3-based ceramics is still required for practical power device applications.

2.2.2. Loss Parameter Introduction

Complex-number parameters were introduced to represent small hysteresis losses in piezoelectrics. Using tanδ′, tanϕ′, and tanθ′ to denote "intensive" dielectric, elastic, and piezoelectric loss factors, respectively, we describe the physical parameters as [28]:

$$\varepsilon^{X*} = \varepsilon^{X}(1 - jtan\delta') \quad (1)$$

$$s^{E*} = s^{E}(1 - jtan\phi') \quad (2)$$

 doi:10.20944/preprints202401.2073.v1

$$d^* = d(1 - jtan\theta') \tag{3}$$

Here j is the imaginary notation, ε^X the dielectric constant under constant stress, s^E the elastic compliance under constant electric field, and d is the piezoelectric constant. The loss tangents are directly related with the degree of hysteresis in the $D-E$, $x-X$ and $x-E$ or $D-X$ curves.

Damjanovic introduced a modified equivalent circuit [29], and Mezheritsky integrated the piezoelectric loss explicitly in their impedance spectrum analysis [30]. In the end of 2000s, a user-friendly formula reported by Zhuang et al. became widely cited for determining these three losses separately from the mechanical quality factors Q_A for resonance and Q_B for antiresonance on the admittance/impedance spectrum curves [31,32]. An example formula for the k_{31} plate mode is expressed as:

$$\begin{cases} Q_{A,31} = \frac{1}{tan\,\phi_{11}'} \\ \frac{1}{Q_{B,31}} = \frac{1}{Q_{A,31}} - \frac{2}{1+(\frac{1}{k_{31}}-k_{31})^2\Omega_{B,31}^{\ 2}}(2\,tan\,\theta_{31}' - tan\,\delta_{33}' - tan\,\phi_{11}') \end{cases} \tag{4}$$

where the resonance- and antiresonance-normalized frequencies

$$\begin{cases} \Omega_{A,31} = \frac{\omega_a l}{2v_{11}^E} = \frac{\pi}{2} \\ \Omega_{B,31} = \frac{\omega_b l}{2v_{11}^E} \end{cases} \tag{5}$$

are interrelated with

$$\begin{cases} \Omega_{A,31} \to v_{11}^E = 1/\sqrt{\rho s_{11}^E} \\ \Omega_{B,31} \to 1 - k_{31}^{\ 2} + k_{31}^{\ 2}\frac{tan\,\Omega_B}{\Omega_B} = 0 \end{cases} \tag{6}$$

Three losses, dielectric, elastic and piezoelectric losses, can be determined separately from the admittance/impedance spectra: (1) from Q_A, $tan\,\phi_{11}'$ is determined, first, (2) $tan\,\delta_{33}'$ is determined from the off-resonance admittance ($j\omega C_d$ and small phase lag), (3) then, from Q_B, $tan\,\theta_{31}'$ can be obtained finally. Note that the experiments in PZT ceramics exhibit the antiresonance mechanical quality factor Q_B always higher than the resonance mechanical quality factor Q_A, leading to a larger tanθ′ than the value of (tanδ′+tanϕ′)/2. To the contrary, it is interesting that $Q_A > Q_B$ was observed in Pb-free piezo-ceramics [33].

[CURRENT ISSUE] The loss mechanism difference, in particular in the piezoelectric loss tanθ′, between the PZT and Pb-free materials should be investigated from the domain dynamics viewpoint.

2.2.3. High-Power Piezoelectric Characterization System (HiPoCS)

The reader probably knows the problem in the voltage-constant admittance measurement with a conventional "impedance analyzer" at the resonance; that is, scewed spectrum peak and spectrum hysteresis with an increase in applied voltage. Thus, current-constant admittance measurement was proposed for obtaining symmetrical spectrum peak [25]. For improving the determination accuracy of Q_A and Q_B simultaneously, a new methodology has been proposed [34]; that is, "voltage/current measurement under constant vibration velocity" with sweeping the frequency. Refer to HiPoCS data shown in Figure 2. During keeping the vibration velocity constant (i.e., stored/converted mechanical energy is constant), the current keeps rather constant and only the voltage shows minimum at the resonance; while the voltage keeps constant and the current shows minimum at the antiresonance frequency. Admittance (ratio current/voltage) and impedance (voltage/current) circles obtained with changing the frequency can provide the mechanical quality factors Q_A and Q_B, respectively, under the same vibration velocity (i.e., mechanical output energy constant). This continous driving measurement is close to the practical device operation condition, that includes temperature rise effect due to heat generation from the loss.

For minimizing the temperature rise of the specimen, "Burst Mode Method" has been proposed by Umeda et al. [35,36] only for the resonance mode Q_A. Shekhani extended the HiPoCS system for measuring also the antiresonance Q_B, in addition to Q_A without changing the system: i.e., 1 ms short

 doi:10.20944/preprints202401.2073.v1

excitation is made at the resonance frequency, then the vibration ring-down is measured under open- or short-circuit conditions [37,38]. This short period excitation does not generate the temperature rise higher than 0.1℃ in the piezo-ceramic specimen. The vibration ring-down rate on the displacement and/or current or voltage under short- or open-circuit conditions can provide the mechanical quality factor Q_A or Q_B, respectively. Note that the ring-down vibration frequencies under Q_A or Q_B are slightly different because of the elastic constant difference, s^E and s^D-like (not D constant, precisely speaking). The benefit of the "Burst Mode Method" includes its quick measurement: one vibration ring-down can be obtained less than 10 seconds, which results in Q_A (or Q_B) as a function of vibration velocity v^{RMS} instantaneously.

[CURRENT ISSUE] The remaining issues in the high-power characterization include the resonance peak spurious problem in the k_{33} and k_{15} mode specimens on the admittance/impedance spectrum due to the mode-coupling, and the sample hoder development not to provide the supporting jig effect on the vibration.

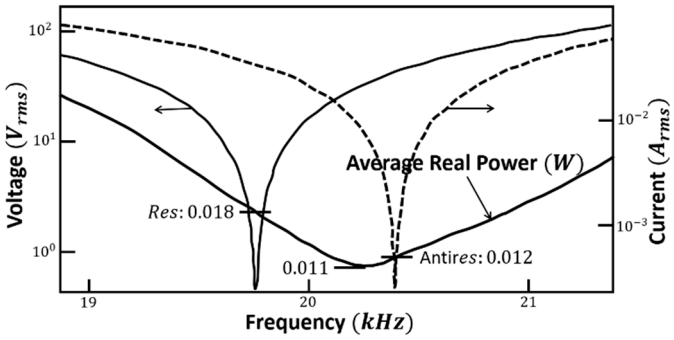

Figure 2. HiPoCS measuring spectrum under constant vibration velocity condition. Voltage shows minimum at the resonance frequency, while current shows minimum at the antiresonance frequency. Note that the required power is minimum at a frequency between the resonance and antiresonance frequency.

2.3. Pb-Free Piezoelectrics

"The Century of Environmental Management" was given for the 21st century. In 2006, European Community started RoHS (Restrictions on the use of certain Hazardous Substances), which explicitly limits the usage of lead (Pb) in electronic equipment. The widely-used PZT piezo-ceramics may be regulated in the future in European, Japanese, and Korean products (except for the US market). This section is related with Global Regulation in Section 5.5.1. Thus, Pb (lead)-free piezoceramics have started to be revived after 1999, which are classified into three types; layered structure (Bi,Na)TiO_3, perovskite type (Na,K)NbO_3 and tungsten bronze.

2.3.1. (Bi,Na)TiO_3

The patents for bismuth compounds (bismuth layered type and (Bi,Na)TiO_3 (BNT) type) share 61% among all Pb-free piezoelectrics. This is owing to easy fabrication of bismuth compounds compared with other compounds. Langevin transducers developed originally for underwater hydrophones and sonars are currently utilized for high-power ultrasonic cleaning and hazardous material dissolving systems. For these ecological applications, it is reasonable to make the systems also environment-friendly. Honda Electronics, Japan developed Langevin transducers with using the BNT based compositions for ultrasonic cleaner applications [39]. $(Bi_{1/2}Na_{1/2})TiO_3$ -$BaTiO_3$ -$(Bi_{1/2}Na_{1/2})(Mn_{1/3}Nb_{2/3})O_3$ ceramics were developed: the electromechanical coupling factor k_t = 0.41 is larger than that of the PZT because of much smaller permittivity ε = 500, despite the small piezoelectric constant d_{33} = 110×10^{-12} C/N, only 1/3 of that of a hard PZT. Furthermore, the v_{max}^{rms} of a k_{31}-mode plate is close to 1 m/s, which is higher than that of typical hard PZTs.

[CURRENT ISSUE] Note that the toxicity of Bi^{3+} is not very low in comparison with Pb^{2+} (closed shell ionic structures of Bi^{3+} and Pb^{2+} are almost the same). However, this atomic element Bi is not

 doi:10.20944/preprints202401.2073.v1

familiar to politicians fortunately, so that they will not propose the regulation. Is this Pb-free composition permitted from your engineering ethics?

2.3.2. $(Na,K)NbO_3$

Perovskite $(Na,K)NbO_3$ (NKN) systems exhibit the highest piezoelectric performance among Pb-free materials because of the morphotropic phase boundary (MPB) usage similar to the PZT system. Toyota Central Research Lab, Japan reported the significant improvement of the piezoelectric properties in the "oriented" ceramics of $(K,Na,Li)(Nb,Ta,Sb)O_3$ [40], where the maximum strain reached up to 1500×10^{-6}, equivalent level to the PZT strain. Their sintering difficulty and the necessity of the sophisticated preparation technique are drawbacks. So-called "topochemical method" was used for preparing flaky raw powders, which were aligned during the green sheet preparation process for making ML structures. Lower mass density and higher heat conductivity of NKN in comparison with the PZTs facilitate them for higher v_{max}^{rms} and higher-power applications [7,41].

[CURRENT ISSUE] Detailed research on heat conductivity of NKN ceramics, in particular composition dependence of heat conductivity, are waiting in order to clarify the physics for high-power density mechanism.

2.3.3. Tungsten-Bronze

Another alternative is Tungsten-bronze (TB) type for high-power density resonance applications, because of its high Curie temperature and low loss. Taiyo Yuden, a Japanese electro-ceramic industry, aimed at disposability for their products. They developed micro ultrasonic motors using Pb-free ML actuators for portable equipment [42]. Their composition was based on tungsten bronze (TB) $(Sr,Ca)_2NaNb_5O_{15}$ without heavy metal or even K (potassium seems to be more toxic scientifically in comparison with Na). Though basic piezoelectric parameters in TB (d_{33} = 55~80 pC/N, T_C= 300℃) were not very attractive, the d_{33} was dramatically enhanced up to 240 pC/N by aligning the *c*-axis orientation. Further the Young's modulus Y_{33}^E = 140 GPa as twice high as that of PZT generates higher stress, which is suitable to ultrasonic motor applications. Taiyo Yuden developed a sophisticated preparation technique for fabricating oriented ceramics with a ML structure: that is, preparation under "strong magnetic field", much simpler than the flaky powder preparation used for the NKN systems. Knowing the diamagnetic property of most of piezo-ceramics, the ceramic powder suspended in slurry is aligned along its magnetically-stable axis under a strong magnetic field (such as 10 T). Because the polarization axis in their particular TB composition corresponds to the magnetically-unstable axis, they chose the magnetic field parallel to the green sheet. A cut-green-sheet was rotated practically under steady magnetic field during drying period.

[CURRENT ISSUE] Refer to a review paper on Pb-free piezoelectrics by Tsurumi [43]. Though Pb-free piezoelectric property is not superior to that of the PZTs in general, the political pressure urges the commercialization efforts on them prior to the expected restriction of the PZT usage. Simple ML devices with "structured ceramics" should be commercialized, in addition to "topochemical ceramic flake" and "strong magnetic field application" preparations.

3. Piezoelectric Actuator Designs

There are several popular designs utilized at present, such as (1) bimorphs / unimorphs, (2) multilayers, (3) monies/cymbals. Recent compact design requirement urges the development of micro-electro-mechanical-systems (MEMSs) on silicon wafers with using piezoelectric thin/thick films.

3.1. Multilayer (ML)Actuators

For manufacturing reliable multilayer actuators, Ag/Pd electrode has been utilized initially in order to suppress the Ag migration problem during pseudo-DC high-voltage operation. However, with miniaturing portable devices in the 21st century, to reduce the driving voltage ML actuators started to be used for high-power AC resonance devices, such as ultrasonic motors and piezo-

 doi:10.20944/preprints202401.2073.v1

transformers. The problem found in these applications was significant Joule heat from the internal electrode due to poor conductivity in Ag/Pd or Pt. Thus, Cu or pure Ag internal electrode (highest conductivity) was required with "hard" PZT ceramic sheets. Ural et al. developed low-temperature-sinterable "hard" PZT, which could be sintered at 900℃ in reduced atmosphere with N_2 [44]. They reported an interesting 40% increase in the maximum power density (at 20℃ temperature rise) on ring-dot disk ML transformers (OD = 27, Center Dot D = 14 mm) with Cu and Ag/Pd (or Ag/Pt) (as references): 42 W/cm^3 and 30 W/cm^3, respectively. This big improvement came merely from the higher electric conductivity of Cu (or pure Ag), compared to Pd or Pt. Note that the power density depends not only on the piezo-ceramic composition, but also on the electrode species particularly in ML designs. Because the capacitance of ML's is large, AC impedance $1/j\omega C_d$ is as low as 10Ω, which is almost comparable to the internal electrode resistance.

[CURRENT ISSUE] Cu-embedded compact ML products are required to be widely commercialized for general customers.

3.2. MEMS Designs

Micro-electro-mechanical-systems have been introduced into piezoelectric actuators in the end of 1990s. For promoting the actuator commercialization, even thin film devices need to be power level higher than 10 mW, in general. Knowing the maximum power density in PZTs 30 W/cm^3, 30 μm is desired for a $3 \times 3\, mm^2$ electrode size. High-power density is realized from both (1) crystallinity enhancement from the polycrystal structure to improve the piezoelectric properties, and (2) volume (or thickness) increase of the piezoelectric film to increase the power level. Du et al. simulated the piezoelectric constant d change in the PZTs with the crystal orientation in 1999 [45], which concluded that a rhombohedral composition exhibits the maximum d_{33}^{eff} and d_{31}^{eff} when the electric field is applied around 71°-cant from the perovskite <1 1 1> polarization direction. That is, the rhombohedral PZT epitaxial film should be deposited as the perovskite [1 0 0] film. The d_{33}^{eff} enhancement is originated from d_{15}, similar to PMN/PT single crystals. Reference [46] verified the higher piezoelectric constant for this crystallographically-canting structure; this structure seems to be a current standard design of commercialized PZT films. PZT epitaxial thick films are deposited on a silicon wafer, which is then micro-machined to leave a membrane for fabricating micro actuators. A blood glucose tester with using 2 – 3 μm PZT films was developed in the end of 1990s by the Penn State University in collaboration with OMRON Corporation, Japan [47]. Two surface interdigital electrodes on the PZT film were driven for exciting membrane waves, which soaked up blood and the test chemical from the two inlets. Then, mixing the liquids in the center part, the mixture was delivered to the detector part through the outlet. Finite Element Analysis (FEA) simulation was conducted to evaluate the flow rate of the liquid by changing the thickness of the PZT or the Si membrane, inlet or outlet nozzle size, and cavity thickness. Because of the enhanced heat dissipation through the Silicon substrate with liquid flow in the thick film chambers, sufficient mechanical power was obtained experimentally for the micro-mixer with only the 2 μm PZT film.

Regarding the sensor applications, much easier than the actuators, submicron thin films can be adopted. Refer to [48] for the piezoelectric MEMS studies.

[CURRENT ISSUE] One of the major problems in the MEMS can be found in the device film membrane design; that is, most of the piezoelectric devices currently developed are based on the "unimorph" structure (submicron PZT film deposited on 100 μm), which shows the lowest electromechanical coupling factor. Various MEMS designs with much higher electromechanical coupling factor k (k_{33} type, or cymbal structure) were proposed in Ref. [8]. Practical realization will be the remaining studies to be conducted.

3.3. AD Preparation Method

In order to realize the practical MEMS actuators with 1 – 10 mW or higher, films thicker than 50 μm are required in mass-production. Aerosol deposition (AD) is a technique for depositing thick ceramic films, better suitable than the sputtering techniques. Akedo et al. developed the AD method, where submicron ceramic particles were accelerated by gas flow, then impacted on a substrate [49,50].

AD can rapidly form a thick, dense, uniform and elastically-hard ceramic layer on almost any substrates (silicon, metal, or even polymer) at room temperature. Using inexpensive and simple production facility, ceramic powders can be solidified without additional heat treatment, even in a low vacuum condition. It is expected to reduce energy and fabrication costs, and to ease thick film preparation with complicated material compositions. Compared to the sputtering (compositional fluctuation problem) or sol-gel spin coating methods (too slow growth rate), the AD method is the most promising technique to realize 30 μm thick PZT films in mass-production scale.

[CURRENT ISSUE] The primary problem of AD is how to enhance the epitaxy of ceramic powder deposition. Even the annealing process is coupled, high epitaxy on a silicon single crystal substrate is difficult thicker than 10 μm.

4. Drive/Control

Since commercially available power supplies have been developed for driving electromagnetic actuators/motors, the output impedance is standardized as resistive $50\,\Omega$, so that 90% of power is bounced back for driving capacitive piezo-actuators under pseudo-DC operation. Thus, special attention is required for drive/control techniques in piezo-actuators for reducing the power supply size. Three types are on-going: (1) negative capacitance power supplies for driving off-resonance piezo-actuators, (2) capacitive AC power supplies for driving resonance piezo-actuators, and (3) DC/DC converters for harvesting electric energy from high-impedance piezoelectric devices.

In the middle of 1980s, after the multilayer actuators became popular, their resonance applications in ultrasonic motors and piezo-transformers required the resistive power supplies with much smaller output impedance, because the impedance of ML actuators (very high capacitance) was as low as $10\,\Omega$ at their resonance. Uchino et al. at NF Corporation developed High Speed Bipolar Amplifier with output impedance less than $1\,\Omega$ and current capability up to 2 A. Refer to [51] for the present product catalog.

4.1. Negative Capacitance Power Supply for Off-Resonance Drive

For capacitive piezoelectric actuators, "energy" flow (real power $V{\cdot}I\cos\varphi$) should be considered rather than "apparent" power flow ($V{\cdot}I$) because of large phase lag. To match the resistive electric impedance of the conventional power supply, a reactive (or inductive) component may be inserted in the driving system in series to the capacitive actuator. However, note that the conventional "coil inductor" kills the size and weight (and Joule loss) in the power supply significantly. Thus, Knowles et al. at Qortek, PA introduced a "negative capacitance" instead of coil in the switching power system [52]. The negative capacitance $-C_p$ equivalent to inductance of $j/\omega C_d$ (C_d: damped capacitance of the piezoelectric device) is inserted in series with the *R-C* power supply circuit. In the case of small electromechanical coupling factor $k = 20\%$ or $k^2 = 4\%$, the power usage will be 2%, then, the remaining 98% will be recovered without losing much as heat in the power system because of the negative capacitance. leading to a high efficiency 98%.

The reader is reminded again that the weakness of inductor *L* is in bulky size and heavy weight, and in electromagnetic noise generation increased a negative capacitance ($-C_p$) usage inevitably.

4.2. Capacitive Power Supply for Optimum Power Condition

Figure 2 shows the HiPoCS measuring spectrum under "constant vibration velocity" condition (see Section 2.2.3). The vibration velocity at the edge of a rectangular plate (k_{31} mode) was maintained with sweeping the frequency from below-resonance to above-antiresonance. Voltage and current show minimum at the resonance and antiresonance, respectively. The required real power, calculated by the product of applied voltage, current and their phase lag, $V{\cdot}I\cos\varphi$, was plotted also in Figure 2. Hirose et al. reported that in comparison with popular resonance drive, the antiresonance drive can reduce the required power in the PZT devices, where $Q_A < Q_B$ [53]. The power supplies for driving the device at both frequencies should be resistive, except for the impedance difference "low" and "high". The mechanical quality factor at any frequency can be calculated from the real electric

 doi:10.20944/preprints202401.2073.v1

power (P_d) and tip vibration velocity (v^{RMS}) as below for a longitudinally vibrating resonator (k_{31}, k_{33}, k_t):

$$Q_m = 2\pi \frac{Energy\ Stored/Cycle}{Energy\ Lost/Cycle} = 2\pi f(\frac{1}{2}\rho {v^{RMS}}^2)/(\frac{P_d}{Lwb}) \quad (7)$$

Shekhani et al. [54] proved first that Q_A and Q_B determined from the voltage and current peak sharpness agree well with the Q_m obtained from Eq. (7) with experimentally obtained P_d (0.018 *W* and 0.012 *W*, respectively) in Figure 2. They pointed out second that the required real power ($V \cdot I \cos \varphi$) exhibits minimum (0.011 *W*) at a frequency between the resonance and antiresonance frequency. In parallel, Shi et al. derived theoretical expectation for this highest efficiency drive frequency [55].

Based on the above speculation, Yuan, Dong et al. developed a new capacitive power supply, with knowing the piezoelectric resonator (Langevin transducer) at the above frequency "inductive" (the phase lag is rather close to – 90 degree) [56,57]. A "Class E Inverter" was designed to drive the transducer at the resonance frequency (resistive) first, with using MATLAB. Then, an impedance converter (basically capacitance C_{cir}) was added for modifying the above Class E inverter driven at the optimum frequency in the inductive region. The optimum driving frequency of this Langevin piezoelectric transducer was f_{opt} = 41.27 kHz in practice, that is between resonance 40.07 kHz and antiresonance frequency 42.05 kHz. The impedance at this frequency was Z_{opt} = 144.2+j2065 (Ω), which is mostly an inductive load. The required electric power (real power $V \cdot I \cos \varphi$) for generating the same vibration velocity at both driving frequencies, resonance (40.07 kHz) and the optimum condition (41.27 kHz) was measured with changing the vibration velocity. The required power for the optimum frequency driving method was reduced by 39% with smaller heat generation, in comparison with that for the resonance frequency driving method, under the vibration velocity $v^{rms} = 53mm/s$. Note that this new driving scheme becomes more attractive with increasing the driving power level (i.e., with an increase in vibration velocity).

4.3. DC/DC Converter

The principle of piezoelectric energy harvesting is to cultivate electrical energy from the environmental mechanical noise vibration via direct piezoelectric effect ($D = dX$). Except for the instantaneous consumption of electrical energy, the obtained energy must be stored in rechargeable batteries. The problem in this process is a significant difference in the electrical impedance: high impedance of the piezoelectric device to low impedance (50 Ω) of the battery. Various converters can step down the voltage to adapt the electrical impedance: Forward converter, Buck Converter, Buck-Boost Converter, Flyback Converter etc. These converters should possess low output impedance and low loss characteristics. As to be described in Section 5.4.1, Kim et al. developed the energy harvesting systems with Cymbal piezo-devices for hybrid cars aiming at the mileage improvement [67,68]. A DC/DC Buck Converter was adopted because of its simplest topology using a single MOSFET (with device loss about 3 mW), which realized power transfer from 53 *mW* at the Cymbal energy harvesting system to 43 *mW* at the converter output (81% efficiency) in practice by converting the original impedance 300 $k\Omega$ down to 5 $k\Omega$ with a 2% duty cycle at a switching frequency of 1 kHz [58,59]. The experimental impedance change 60 times above differed from the expectation 2500 times, that may be explained by the other components' losses in the circuit.

[CURRENT ISSUE] Though we find many papers on the energy harvesting less than 1 *mW*, the reader is reminded that the energy collection less than 10 *mW* is not a useful technology, because it cannot be stored in a rechargeable battery due to a couple of *mW* inevitable circuit loss.

5. Piezoelectric Actuator Applications

The applications of piezoelectric actuators in the 21st century seem to be oriented toward "politico-engineering" with four keywords, "cooperation, protection, reduction, and continuation". This section introduces typical such examples.

 doi:10.20944/preprints202401.2073.v1

5.1. Sustainability Technologies - Cooperation

5.1.1. Global Technological Regulations

International agreements are being set in the regulations on toxic materials, environmental contaminants (such as CO_2), "Non-Proliferation of Nuclear Weapons", and international standardization of electrical and computer systems (such as World Wide Web, and Global Positioning System). Accordingly, international "cooperation" on piezoelectric developments may be found in: (1) Pb-free materials (already explained in Section 2.3), (2) earthquake monitoring equipment, and (3) landmine detectors.

5.1.2. Elimination of Hazardous Wastes

Industrial ultrasonic cleaners are widely utilized in the manufacturing lines of Silicon wafers and liquid crystal display glass substrates. Increasing the ultrasonic power level in water generates so-called "cavitation" that is vacuum particle in water. Because the cavitation effect is equivalent to cyclic adiabatic compression and expansion at around 28 kHz, it also generates micro-local heating more than 3,000°C for a short period, which makes some hazardous waste innocuous. In the late 20th century, various hazardous wastes have been produced underground or in sewer water, including dioxin, trichloroethylene, PCB, environmental hormone etc. [5]. It is well known that "dioxin" becomes another toxic material when it is burned at a low temperature in typical garbage disposal furnaces; while it becomes innocuous only when burned at a high enough temperature. Ultrasonic irradiation is highly prospected for this application. So-called "Sono-Chemistry" induced in water dissolves dioxin into innocuous materials without increasing whole water temperature apparently [60].

[CURRENT ISSUE] Government-initiated cooperative actions will be urged immediately, in parallel to Global Warming Protection Agreement.

5.2. Crisis Technologies - Protection

There are five types of crises [5]:

1. Natural disasters (earthquakes, tsunamis, tornadoes, hurricanes, lightning, etc.),
2. Epidemic/infectious diseases (smallpox, polio, measles, HIV, and COVID19),
3. Enormous accident (Three-Mile-Island uranium core meltdown, BP oil spill etc.),
4. Intentional accidents (acts of terrorism, criminal activity, etc.),
5. Civil-war, war, territorial aggression.

5.2.1. Epidemic/Infectious Disease

- Biosensor

The reader knows that COVID-19 detecting sensors have been developed immediately after the onset in 2019. The principle of micro-mass sensors fabricated with Quartz is high monitoring resolution of resonance frequency $\Delta f_R/f_R \sim 10^{-6}$, owing to the large mechanical quality factor $Q_m \sim 10^6$. A specific antibody/phage is coated on a single crystal quartz oscillator. Once particular bacteria are captured selectively by the antibodies, the surface mass of the oscillator is increased. Thus, small mass change can be finely detected through the resonance frequency shift. This micro-mass sensor was utilized as a bio-sensor by Cheng in 2003 [61] for detecting bacteria, such as E. Coli and Salmonella. Since 10^4~10^7 cells per *ml* is already critical to humans for Salmonella's case, a mass-sensitivity corresponding to 10^4 cells per *ml* was already achieved.

- Bacteria/Virus Disinfector

On the other hand, sensing was not enough against the Anthrax attack by the terrorists in 2001. In order further to "neutralize" the biological attack, a portable hypochlorous-acid disinfection device was developed in 2003 by Pezeshk et al. at The Penn State University, with using a piezoelectric

 doi:10.20944/preprints202401.2073.v1

ultrasonic humidifier [62]. Hypochlorous Acid is well-known disinfectant with no side effects on humans, thus, would be ideal for disinfection of office and hospital buildings against viruses like SARS, Anthrax, and COVID 19. Disinfection effects can be enhanced with fine mist of the acidic solution. However, the acid is not sold as a pure solution since it naturally disintegrates after a few hours. They designed a portable corrosion resistant electrolytic cell to produce hypochlorous acid from "brine". Nafion® membranes were used to separate, then produce hypochlorous acid and sodium hydroxide in the anode and cathode compartments, respectively. Commercialized ultrasonic piezoelectric atomizer was modified to corrosion-resistive, then utilized to generate micro-droplets of the diluted acid.

5.2.2. Anti-Terrorism Technologies

The reader may feel frustrated when airport security removes what is no more than a bottle of water from your carry-on baggage at the checkpoint every time. This is because the X-ray system cannot distinguish water from "liquid bombs", such as NTN (nitroglycerin and triacetone-triperoxide). In collaboration with Micromechatronics, Inc., PA, Lawrence Livermore National Laboratory (LLNL), CA developed a Gamma-ray scan inspection system, which can distinguish atomic species, i.e., distinguish liquid explosives from water. As the reader knows, Gamma-rays are the highest-energy form of electromagnetic radiation, due to their shorter wavelength than the X-ray, leading to higher resolution on atomic species. A compact "neutron accelerator" is required for a "Gamma ray spectroscopy" as a high-energy photon source. The key to this system is a miniaturized very-high voltage supply (1 M*V*) to accelerate a neutron beam. Micromechatronics, Inc. utilized a multilayer piezoelectric transformer with output capability of 1~10 kV-AC, which was combined with a Cockcroft Multiplier Circuit to obtain 10~100 kV-DC with 85% efficiency. Cascading 3~10 of these 100 kV-DC supply units, they reported 300 kV~1 MV final voltage [5].

5.2.3. Intentional Accident/War

Weapon development for mass destruction was the conventional focus, including nuclear bombs and chemical weapons. However, based on the global trend for "Jus in Bello (Justice in War)" in the 21st century, environment-friendly "green" weapons became the main-stream; that is, minimal destructive weapons with a pin-point target such as laser guns and rail guns. In this direction, during the revenge war against the World Trade Center terrorists, the development of programmable air-bust munition (PABM) was encouraged by the US Army in 2004. The 25 mm caliber "Programmable Ammunition" by ATK Integrated Weapon Systems, AZ and Micromechatronics, PA [63] installed a micro-processor in each own bullet, in order to explode itself at the programmed position, so that the bullet could kill only the inside terrorists without collapsing the building. Because a button battery was deteriorated easily in the severe-weather battlefield, a multilayer piezo-device was newly adopted for generating electric energy under shot impact. This harvested energy activated the operational amplifier which ignited the burst according to the command program without impact fuse. This is one of the million-selling piezo-energy harvesting devices at present.

5.3. Crisis/Sustainability Technologies - Reduction

5.3.1. River Contaminant Reduction

Detergent and shampoo are two of the regular causes of the river contamination. In collaboration with Honda Electronics, Sharp, Japan produced washing machines with an ultrasonic stain remover in 2003. The L-L coupler horn was utilized to generate water cavitation which removes oily dirt from a shirt collar, and muddy dirt from sportwear. Thus, we can reduce the amount of detergent significantly by this ultrasonic technique. Ref [64] shows present versions of the portable stain remover.

 doi:10.20944/preprints202401.2073.v1

5.3.2. Reduction of Contamination Gas

Diesel engines are recommended rather than regular gasoline cars from the energy conservation and global warming viewpoint. Let us consider the total energy of gasoline production; "well-to-tank" and "tank-to-wheel". The energy efficiency, measured by the total energy required for unit drive distance for a vehicle (MJ/km) (i.e., "tank-to-wheel"), is of course better for high octane gasoline than diesel oil. On the other hand, since the electric energy required for purification is significant (i.e., "well-to-tank"), the diesel is superior to gasoline.

As well known, however, the conventional diesel engine generates toxic exhaust gases such as SO_x and NO_x. In order to solve this problem, new diesel injection valves (so-called common rail type diesel injection valve) were developed by worldwide manufacturers, Siemens, Bosch and Toyota with piezoelectric ML actuators [65].

For satisfying both requirements, elimination of toxic SO_x and NO_x and increase in the diesel engine efficiency, high injection pressure and quick valve control (0.1 ms) are required for generating fine mist of diesel fuel in the common rail type. Because of the performance limitation in force and response speed of the electromagnetic actuators, piezoelectric ML actuator should be adopted. The reliability of the ML actuator at an elevated temperature (150°C in engine surrounding) for a long period (10 years) achieved satisfied automobile's specifications [65]. The piezoelectric actuator is a key component to realize (1) high burning efficiency and (2) toxic exhaust gas minimization.

5.4. Sustainability Technologies - Continuation

5.4.1. New Energy Harvesting Systems

Piezoelectric energy harvesting development started in the 1990s, then recent studies focuses on more practical commercialization, as described in Section 5.2.3 [8]. Environmental mechanical noise vibration generates cyclic electric field in the piezoelectric device. The author suggested that the target of "piezo energy harvesting" should NOT be aligned on the large energy cultivation line ($MW \sim GW$) such as windmills and solar cells, but be set on "elimination of batteries". Though used batteries are classified as "hazardous wastes", recycling rate is less than 0.5% of 10s billion batteries sold per year in the world. From this sense, we propose the "piezo energy harvesting" is one of very important technologies in the current "Sustainable Society" from this hazardous waste (batteries) elimination viewpoint.

- Instantaneous Usage

Various instantaneous-usage applications have already been commercialized, in addition to PABM for the 25 $mm\phi$ bullet. NEC-Tokin developed an LED traffic light array system driven by a piezoelectric windmill, which is operated by wind generated effectively from running automobiles on freeways in Hokkaido (northern island in Japan). Successful million-selling products off the shelf include "Lightning Switch", remote switch for room lights, with using a unimorph piezoelectric component commercialized by PulseSwitch Systems, VA [66]. Remote switch adds living convenience first, furthermore can reduce the housing construction cost by up to 30% due to a significant reduction of the copper electric wire and the aligning labor.

- Continuous Harvesting System

Another category of energy harvesting systems is to accumulate electric energy in a rechargeable battery. There are three major phases in the piezoelectric energy harvesting process [8]: (i) mechanical-mechanical energy transfer: mechanical stability of the piezoelectric transducer under large stresses, and mechanical impedance matching, (ii) mechanical-electrical energy transduction: the electromechanical coupling factor in the composite transducer structure, and (iii) electrical-electrical energy transfer: electrical impedance matching with a DC/DC converter. The Penn State group developed energy harvesting piezoelectric devices based on a "Cymbal" structure (29 mmϕ, 1-2 mm thick), which can generate electric energy up to 100 mW under an automobile engine vibration [67,68]. By combining three cymbals in a rubber composite, a washer-like energy harvesting

 doi:10.20944/preprints202401.2073.v1

sheet was developed for a hybrid car application, aiming at 1*W*-level constant accumulation to a fuel cell.

5.4.2. Medical Acoustic Probes

Two types of piezoelectric transducers are used in ultrasonic imaging systems. First, mechanical sector transducers consisting of a single resonator can provide images by mechanical resonator scanning such as wobbling. Second, multiple element array transducers possess discrete elements that are accessed individually by the imaging system so as to enable electronic focusing on the scanning plane to various adjustable penetration depths through the use of phase delays. Array transducers are categorized further two types: linear and phased (or sector).

- Linear Array

A linear array is a collection of elements arranged in one direction, producing a rectangular display. A curved linear (or convex) array is a modified linear array whose elements are arranged along an arc to permit an enlarged trapezoidal field of view. The elements of these linear-type array transducers are excited sequentially group by group with the sweep of the beam in one direction. These linear array transducers are used for radiological and obstetrical examinations.

- Phased Array

A phased array transducer steers the acoustic beam by signals applied on the elements with delays, for creating a sector display. This transducer is useful for cardiology applications where positioning between the ribs is necessary [4].

Toshiba Corporation, Japan developed a medical imaging transducer with adopting the superiority of the PZN–PT single crystal to the PZT ceramics; much higher electromechanical coupling factor k_{33} (or k_t) [69]. The medical doctor needs to use two different conventional PZT probes with narrow bandwidth; one is 2.5 MHz for checking wider and deeper area, and the other is 3.75 MHz for monitoring the specified area with a better resolution. To the contrary, the new probe with the PZN–PT single crystal (with cant crystallographic orientation as introduced in the beginning of Section 2) can cover wide bandwidth without changing the probe; that is, the doctor can just switch the drive frequency from 2.5 to 3.75 M*Hz*. High k_{33} and k_t characteristic provides merits: (1) wide bandwidth, (2) high image resolution, and (3) strong signal—because of the high k_{33} and k_t, the receiving signal level is enhanced more than double in comparison with the PZT probe, leading to the penetration depth enhancement [69].

5.4.3. Micro-Disrupter for Medical Catheter Applications

The Penn State University has developed various micro rotary motors (1 - 5 mm in size) [70,71]. A micro motor called “metal tube type” consists of a metal hollow cylinder and two (or four) PZT rectangular plates bonded on the metal tube surface. When one of the PZT plates is operated, a bending vibration of the composite tube is excited. However, because of an asymmetrical mass of another non-excited PZT plate, another hybridized bending mode is excited with some phase lag, leading to an elliptical locus of the metal tube in a clockwise direction, like a Hula-Hoop motion. A pair of stainless ferrule were pressed onto the both ends of wobbling metal tube with a spring. The metal cylinder motor 2.4 mm in diameter and 12 mm in length was driven at 62.1 kHz in both rotation directions. They reported the motor specs: no-load speed of 1800 rpm and an output torque up to 1.8 *mN·m* in both direction rotation under an applied *rms* voltage of 80 V. Rather high maximum efficiency of 28% for this small motor is a noteworthy feature.

In collaboration with the Penn State University, Samsung Electromechanics, Korea, developed the world-first camera module with both optical zooming and auto focusing mechanism for a cellular phone application in 2003 [72]. The reader may remember that two metal-tube ultrasonic motors with 2.4 mm diameter and 14 mm length were installed to control zooming and focusing lenses independently in conjunction with screw mechanisms, which have been modified in the new Galaxy Smartphones [73].

 doi:10.20944/preprints202401.2073.v1

Micro motors less than 1.3 mmϕ with 3 mm long are very useful for the micro surgery or minimal invasive surgery. Micromechatronics Inc., PA, in collaboration with the Penn State University, developed "Micro-Disrupter™" by combining the metal tube motor with a drill, as illustrated in Figure 3 [74]. Coupled with a medical catheter, the drill could disrupt big blood clot successfully, which may help the brain cerebral infarction or heart stroke patient even on an ambulance.

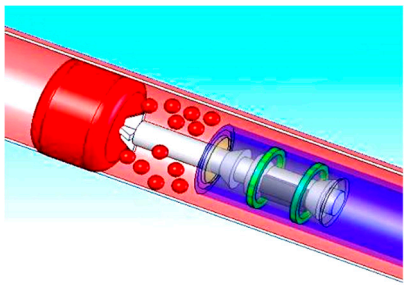

Figure 3. Medical catheter application for blood clot removal, using a "metal-tube" motor [74]. The motor is composed of a metal tube with two rectangular PZT plates bonded on the tube.

6. Conclusions

The author proposed that the incident, terrorist attack on the US in the beginning of the 21st century created symbolically the "Politico-Engineering" strategy; that is, strong political initiative is required for promoting the engineering development. The author comments on the paradigm shift from "econo-engineering" to politico-engineering in Science & Technology development. In the 1980s, i.e., "Bubble Economy" period, cost/performance technologies were sought with the governmental slogan, "lighter, thinner, shorter, smaller (軽薄短小)"; while in the 2000s, sustainability and crisis technologies should be the mainstream along the slogan "cooperation, protection, reduction, continuation (協守減維)". These trendy technologies are primarily initiated by the political regulations.

As already introduced, the crisis includes:

(1) natural disaster,
(2) infectious/contagious disease,
(3) enormous accident,
(4) intentional terrorist/criminal incident, and
(5) external & civil war/territorial invasion.

To the contrary, the sustainability technologies were introduced on the following piezoelectric device areas, including medical applications:

(a) non-toxic Pb-free piezo-materials,
(b) ultrasonic disposal technology for hazardous materials,
(c) reduction of contamination gas with piezo-devices,
(d) new energy source creation (i.e., piezoelectric energy harvesting), and
(e) energy-efficient piezoelectric device development.
(f) medical acoustic probes, micro-disrupters for medical catheters

This article proposed a new four-Chinese-character slogan for the era of "politico-engineering", "協, 守, 減, 維 (cooperation, protection, reduction, and continuation)". Standardization of internet systems and computer cables require global "cooperation" and coordination to accelerate the mutual communication. The "Paris Agreement" in 2016 is an international agreement on "Greenhouse Gas" regulation linked to the United Nations Framework Convention on Climate Change. "Protection" is mandatory for the territory and environment from the enemy or natural disaster, and for pandemic disease spread. "Reduction" of toxic materials and energy consumption should be urged, then the society "continuation" (or sustainable society) in parallel with the medical technology advancement will be an ultimate desire.

Finally, for the junior product developer's sake, let me explain the difference among the product planning strategies for techno-, economic-, and politico-engineering cases, as illustrated in Figure 4

 doi:10.20944/preprints202401.2073.v1

[75]. As exemplified by the "discovery" of single crystal relaxor-piezoelectrics, the techno-engineering starts from the fundamental science and technology (S&T) or the discovery, then its performance development follows. Finally application products are created. The econo-engineering, as exemplified by the "invention" of piezo-multilayer components, starts from the final product specs, in mass-production capability and manufacturing cost in the ML case. Based on these desired specs, manufacturing processes are developed as the key technology. The fundamental S&T is sought only when required. To the contrary, as in the case of Pb-free piezoelectrics, the politico-engineering is brought in with the legal regulation. The final products specs should be set first with strict constraints in terms of law-issuing date, performance regulation. For instance, Pb fraction in the final product, CO_2, NO_x, or SO_x emission amount, specifications for rescue robots and new "green" weapons are determined by politicians. In the case of the automobile diesel injection valve, the next step includes the multilayer actuator development as the key for providing the solution. Furthermore, in the RoHS regulation on the PZT, we need to find new suitable Pb-free piezoelectric materials in the fundamental S&D domain. Note that the product planning strategy is totally opposite in Politico-Engineering case in the 21st century from that in Techno-Engineering case in the late 20th century.

The author wishes coming-in researchers to follow the above "product planning strategy" efficiently in studying on the [CURRENT ISSUE]'s suggested in this article.

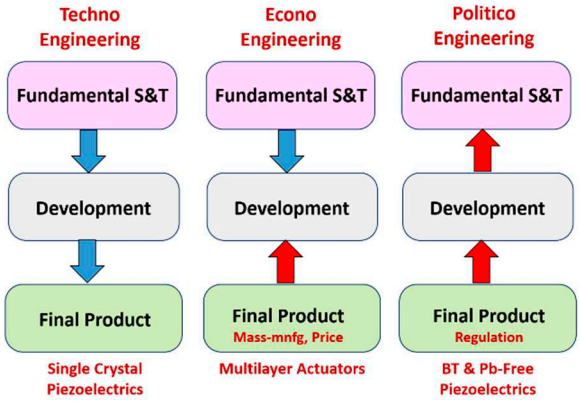

Figure 4. Difference among the product planning strategies for "Techno-Engineering", "Econo-Engineering", and "Politico-Engineering".

Funding: The individual research contents have been supported by various funds from the US Office of Naval Research. N00014-91-J-4145, 92-J-1510, 96-1-1173, 99-1-0754, 08-1-0912, 12-1-1044, 17-1-2088, and 20-1-2309.

Data Availability Statement: Data will be made available on request.

Acknowledgments: The author express his sincere gratitude for the research support from the US Office of Naval Research through Grants # N00014-91-J-4145, 92-J-1510, 96-1-1173, 99-1-0754, 08-1-0912, 12-1-1044, 17-1-2088, and 20-1-2309.

Conflicts of Interest: The author declares no conflict of interest.

References

1. Uchino, K. Essentials for Developments and Applications of Piezoelectric Actuators, Electronics Essentials Series No. 3, Japan Industrial Technology Center, Tokyo, Japan (1984). [In Japanese]
2. Uchino, K. Piezoelectrics/Electrostrictive Actuators, Morikita Pub. Co., Tokyo, Japan (1986). [In Japanese]
3. Uchino, K. Piezoelectric Actuators and Ultrasonic Motors, Kluwer Academic Publishers, Norwell, MA (1997). ISBN: 0-7923-9811-4..
4. Uchino, K. Ferroelectric Devices 2nd Edition, CRC Press, NY (2009). ISBN 978-1-4398-0375-2
5. Uchino, K. Global Crisis and Sustainability Technologies, World Scientific Pub., Toh Tuck Link, Singapore (2017). ISBN: 978-981-3142-29-9.

6. Uchino, K. Micromechatronics Second Edition, CRC Press, Boca Raton, FL (2020). ISBN-13: 978-0-367-20231-6.
7. Uchino, K. High-Power Piezoelectrics and Loss Mechanisms, CRC Press, Boca Raton, FL (2020). ISBN-978-0-367-54069-2.
8. Uchino, K. Essentials of Piezoelectric Energy Harvesting, World Scientific, Singapore (2021). ISBN: 9789811234637.
9. Sawaguchi, E. Ferroelectricity versus antiferroelectricity in the solid solutions of $PbZrO_3$ and $PbTiO_3$, J. Phys. Soc. Japan, Vol. 8, pp. 615-629 (1953).
10. Jaffe, B. Piezoelectric transducers using lead titanate and lead zirconate, US Patent 2,708,244, May (1955).
11. Cross, L. E., S. J. Jang, R. E. Newnham, S. Nomura, and K. Uchino, Large electrostrictive effects in relaxor ferroelectrics, Ferroelectrics, vol. 23, no. 1, pp. 187–191 (1980).
12. Uchino, K., S. Nomura, L. E. Cross, S. J. Jang, and R. E. Newnham, Electrostrictive effect in lead magnesium niobate single crystals, J. Appl. Phys., vol. 51, no. 2, pp. 1142–1145 (1980).
13. Uchino, K., S. Nomura, L. E. Cross, R. E. Newnham, and S. J. Jang, Electrostrictive effect in perovskites and its transducer applications, J. Mater. Sci., vol. 16, no. 3, pp. 569–578 (1981).
14. Uchino, K. Electrostrictive and Piezoelectric Effects in Relaxor Ferroelectrics: Historical Background, IEEE UFFC Transactions Vol. 69, No. 11, pp. 3165002 (2022).
15. Wada, B. Hubble Telescope Structure, JPL document D-10659, pp. 23, (1993).
16. Kuwata, J., K. Uchino and S. Nomura, Phase Transitions in the Pb $(Zn_{1/3}Nb_{2/3})O_3$-$PbTiO_3$ System, Ferroelectrics, 37, pp. 579 (1981).
17. Kuwata, J., K. Uchino and S. Nomura, Dielectric and Piezoelectric Properties of 0.91Pb(Zn1/3Nb2/3)O3-0.09PbTiO3 Single Crystals, Jpn. J. Appl. Phys., Vol. 21, pp. 1298 (1982).
18. Davis, M., M. Budimir, D. Damjanovic, and N. Setter, Rotator and Extender Ferroelectrics: Importance of the Shear Coefficient to the Piezoelectric Properties of Domain-Engineered Crystals and Ceramics, J. Appl. Phys., vol. 101, no. 5 (2007) Art. no. 054112, doi: 10.1063/1.2653925.
19. Yanagisawa, K., H. Kanai, and Y. Yamashita, Hydrothermal Crystal Growth of Lanthanum-Modified Lead Zirconate Titanate, Japan. J. Appl. Phys., vol. 34, no. 9B, pp. 536 (1995).
20. S.-E. Park, S.-E, and T. R. Shrout, Ultrahigh Strain and Piezoelectric Behavior in Relaxor Based Ferroelectric Single Crystals, J. Appl. Phys., vol. 82, no. 4, pp. 1804–1811 (1997).
21. Yamamoto, N., Y. Yamashita, Y. Hosono, K. Itsumi, and K. Higuchi, Method of Manufacturing Ultrasonic Probe and Method of Manufacturing Piezoelectric Transducer, U.S. Patent 0 062 261 A1 (2014).
22. Sun, Y., T. Karaki, T. Fujii, and Y. Yamashita, Enhanced Electric Property of Relaxor Ferroelectric Crystals with Low AC Voltage High Temperature Poling, Jpn. J. Appl. Phys., vol. 59, no. SP, Nov. (2020). Art. no. SPPD08, doi: 10.35848/1347-4065/abb2ff.
23. Qiu, C., J. Liu, F. Li, and Z. Xu, Thickness Dependence of Dielectric and Piezoelectric Properties for Alternating Current Electric-Field-Poled Relaxor-$PbTiO_3$ Crystals, J. Appl. Phys., vol. 125, no. 1, Jan. (2019). Art. no. 014102, doi: 10.1063/1.5063682.
24. Qiu, C. et al., Transparent Ferroelectric Crystals with Ultrahigh Piezoelectricity, Nature, vol. 577, no. 7790, pp. 350–354, Jan. (2020).
25. Hirose, S., M. Aoyagi, Y. Tomikawa, S. Takahashi, and K. Uchino, High Power Characteristics at Antiresonance Frequency of Piezoelectric Transducers, Ultrasonics, 34, pp. 213-217 (1996).
26. Ryu, J., H. W. Kim, K. Uchino and J. Lee, Effect of Yb Addition on the Sintering Behavior and High Power Piezoelectric Properties of $Pb(Zr,Ti)O_3$-$Pb(Mn,Nb)O_3$, Japan. J. Appl. Phys., 42(3), 1307-1310 (2003).
27. Gao, Y., K. Uchino and D. Viehland, Rare Earth Metal Doping Effects on the Piezoelectic and Polarization Properties of $Pb(Zr,Ti)O_3$-$Pb(Sb,Mn)O_3$ Ceramics, J. Appl. Phys. Vol. 92, pp. 2094-2099 (2002).
28. Uchino K. and Hirose S. Loss Mechanisms in Piezoelectrics: How to Measure Different Losses Separately, IEEE Trans. Ultrason. Ferroelectr. Freq. Control Vol. 48, pp. 307-321 (2001).
29. D. Damjanovic, D. An Equivalent Electric-Circuit of a Piezoelectric Bar Resonator with a Large Piezoelectric Phase-Angle, Ferroelectrics. Vol. 110, pp. 129–135 (1990).
30. Mezheritsky, A. V. Efficiency of Excitation of Piezoceramic Transducers at Antiresonance Frequency, IEEE Trans. Ultrasonics, Ferroelectrics, and Frequency Control, 49(4), pp. 484-494 (2002).
31. Zhuang, Y., S. O. Ural, A. Rajapurkar, S. Tuncdemir, A. Amin, and K. Uchino, Derivation of Piezoelectric Losses from Admittance Spectra, Japan. J. Appl. Phys., 48, p.041401 (2009).

32. Zhuang, Y., S. O. Ural, S. Tuncdemir, A. Amin, and K. Uchino, Analysis on Loss Anisotropy of Piezoelectrics with ∞mm Crystal Symmetry, Japan. J. Appl. Phys., 49, p. 021503 (2010).
33. Gurdal, E. A., S. O. Ural, H. Y. Park, S. Nahm, and K. Uchino, High Power Characterization Of $(Na_{0.5}K_{0.5})NbO_3$ Based Lead-Free Piezoelectric Ceramics, Sensors and Actuators A: Physical Vol. 200, pp. 44 (2013).
34. Ural, S. O., S. Tuncdemir, Y. Zhuang and K. Uchino, Development of a High Power Piezoelectric Characterization System (HiPoCS) and Its Application for Resonance/Antiresonance Mode Characterization, Jpn. J. Appl. Phys., Vol. 48, 056509 (2009).
35. Umeda, M., K. Nakamura and S. Ueha, Effects of Vibration Stress and Temperature on the Characteristics of Piezoelectric Ceramics under High Vibration Amplitude Levels Measured by Electrical Transient Responses, Jpn. J. Appl. Phys., Vol. 38, 3327-3330 (1999).
36. Takahashi, S., Y. Sasaki, M. Umeda, K. Nakamura, and S. Ueha, Characteristics of piezoelectric ceramics at high vibration levels, MRS Proceedings. 604, 15 (1999).
37. Shekhani, H., T. Scholehwar, E. Hennig, and K. Uchino, Characterization of Piezoelectric Ceramics Using the Burst/Transient Method with Resonance and Antiresonance Analysis, J. Am. Ceram. Soc., 1–10 (2016). DOI: 10.1111/jace.14580
38. Uchino, K., Y. Zhuang, and S. O. Ural, Loss Determination Methodology for a Piezoelectric Ceramic: New Phenomenological Theory and Experimental Proposals, J. Adv. Dielectrics, 1, No. 1, 17-31 (2011).
39. Tou, T. Y. Hamaguchi, Y. Maida, H. Yamamori, K. Takahashi and Y. Terashima, Properties of $(Bi_{0.5}Na_{0.5})TiO_3$–$BaTiO_3$–$(Bi_{0.5}Na_{0.5})(Mn_{1/3}Nb_{2/3})O_3$ Lead-Free Piezoelectric Ceramics and Its Application to Ultrasonic Cleaner, Jpn. J. Appl. Phys., Vol. 48, 07GM03 (2009).
40. Saito, Y., Takao, H., Tani, T., Nonoyama, T., Takatori, K., Homma, T., Nagaya, T., Nakamura, M. Lead-Free Piezo Ceramics, Nature 432(7013), 84-7 (2004). DOI: 10.1038/nature03028.
41. Gurdal E. A., S. O. Ural, H. Y. Park, S. Nahm, and K. Uchino, High Power Characterization of $(Na_{0.5}K_{0.5})NbO_3$ Based Lead-Free Piezoelectric Ceramics, Sensors and Actuators A: Physical Vol. 200, pp. 44 (2013).
42. Doshida, Y. Bi-Tungsten Piezoceramics, Proc. 81st Smart Actuators/Sensors Study Committee, JTTAS, Dec. 11, Tokyo (2009).
43. Tsurumi, T., Pb-free Piezoelectric Ceramics, J. Japan. Ceramic Soc., p. 40 (2005).
44. Ural, S., S. –H. Park, S. Priya and K. Uchino, High Power Piezoelectric Transformers with Cofired Copper Electrodes- Part I, Proc. 10th Int'l Conf. New Actuators, Bremen, Germany, June 14-16, 2006, P23, p. 556-558 (2006).
45. Du, X. H., Q. M. Wang, U. Belegundu and K. Uchino, Piezoelectric Property Enhancement in Polycrystalline Lead Zirconate Titanate by Changing Cutting Angle, J. Ceram. Soc. Jpn., 107 (2), 190 - 191 (1999).
46. Kalpat, S., X. Du, I. R. Abothu, A. Akiba, H. Goto and K. Uchino, Effect of Crystal Orientation on Dielectric Properties of Lead Zirconate Titanate Thin Films Prepared by Reactive RF-Sputtering, Jpn. J. Appl. Phys., 40, 713-717 (2001).
47. Kalpat, S., Ph.D. Thesis, Penn State Univ., Fall (2001).
48. Tadigadapa S., and K Mateti, Piezoelectric MEMS sensors: state-of-the-art and perspectives, Meas. Sci. Technol., 20, 2009, 092001.
49. Akedo, J. Advanced Piezoelectric Materials (Ed. by K. Uchino), Chapter 14 Aerosol Techniques for Manufacturing Piezoelectric Materials, pp. 493, Woodhead Pub., Cambridge, UK (2010).
50. Akedo, J., Ryu, J., Jeong, D. -Y., Johnson, S. D. Chapter 15 Aerosol Deposition (AD) and Its Applications for Piezoelectric Devices, Advances Piezoelectric Materials - Science and Technology 2nd Edition, Ed. by K. Uchino, pp. 575, Woodhead Pub./Elsevier Ltd., Cambridge, UK (2017).
51. https://www.nfcorp.co.jp/english/pro/pp/p_amp/h_spe/hsa_s/index.html
52. http://www.qortek.com/en/products/piezo-drivers/polydrive-low-cost-lab-driver/
53. Hirose, S., S. Takahashi, K. Uchino, M. Aoyagi and Y. Tomikawa, Measuring Methods for High-Power Characteristics of Piezoelectric Materials, Proc. MRS '94 Fall Mtg., Vol. 360, p. 15 (1995).
54. Shekhani, H. N., and K. Uchino, Evaluation of the mechanical quality factor under high power conditions in piezoelectric ceramics from electrical power. J. European Ceramic Society 35 (2), 541-544 (2014).
55. Shi, W., H. Zhao, J. Ma, Y. Yao, and K. Uchino, Investigating the Frequency Spectrum of Mechanical Quality Factor for Piezoelectric Materials Based on Phenomenological Model, Jpn. J. Appl. Phys. 54, 101501 (2015).

56. Yuan, T., X. Dong, H. Shekhani, C. Li, Y. Maida, T. Tou and K. Uchino, Driving an Inductive Piezoelectric Transducer with Class E Inverter, Sensors & Actuators A: Physical, A261, 219 (2017).
57. Dong, X., T. Yuan, M. Hu, H. Shekhani, Y. Maida, T. Tou, and K. Uchino, Driving frequency optimization of a piezoelectric transducer and the power supply development, Rev. Sci. Instruments 87, 105003 (2016). doi: 10.1063/1.4963920
58. Kim, H. -W., S. Priya, and K. Uchino, Modeling of Piezoelectric Energy Harvesting Using Cymbal Transducers, Japan. J. Appl. Phys. 45, pp. 5836 (2006).
59. Kim, H. -W., S. Priya, H. Stephanau and K. Uchino, Consideration of Impedance Matching Techniques for Efficient Piezoelectric Energy Harvesting, IEEE Trans. UFFC, 54, pp. 1851 (2007).
60. Stavrescu R., Kimura T., Fujita M., Sohmiya H., Ando T., Vinatoru M. Ultrasonic Degradation of a Dioxin-type Molecule, Bulletin of Shiga University of Medical Science (General Education) 11, pp. 15-21 (2001).
61. Cheng, Z. -Y. Private Communication, Auburn University (2003).
62. Pezeshk, A., Y. Gao and K. Uchino, Ultrasonic Piezoelectric Hypochlorous Acid Humidifier for Disinfection Applications, NSF EE REU Penn State Annual Research Journal Vol. II, ISBN 0-913260-04-5 (2004).
63. "http://www.atk.com/MediaCenter/mediacenter_ video gallery.asp" is not available at present. Refer to K. Uchino, Proc. New Actuator 2010, A3.0, Bremen, Germany, June 14-16 (2010).
64. https://www.amazon.com/SHARP-washing-machine-Ultrasonic-Warranty/dp/B01K1DHC2Y
65. Fujii, A., Diesel Injection Valve Control by Piezoelectric Multilayer Actuators, Proc. Smart Actuators/Sensors Study Committee, JTTAS, Dec. 2, Tokyo (2005).
66. http://www.lightningswitch.com/
67. Kim, H. -W., S. Priya, K. Uchino and R. E. Newnham, Piezoelectric Energy Harvesting under High Pre-stressed Cyclic Vibrations, J. Electroceramics, Vol. 15, 27-34 (2005).
68. Kim, H. -W., S. Priya, and K. Uchino, Modeling of Piezoelectric Energy Harvesting Using Cymbal Transducers, Jpn. J. Appl. Phys. Vol. 45, 5836-5840 (2006).
69. Saitoh, S., T. Takeuchi, T. Kobayashi, K. Harada, S. Shimanuki and Y. Yamashita, An Improved Phased Array Ultrasonic Probe Using 0.91Pb($Zn_{1/3}Nb_{2/3}$)O_3–0.09$PbTiO_3$ Single Crystal, Jpn. J. Appl. Phys., 38(5B), 3380–3384 (1999).
70. Koc, B., S. Cagatay and K. Uchino, A Piezoelectric Motor Using Two Orthogonal Bending Modes of a Hollow Cylinder, IEEE Ultrasonic, Ferroelectric, Frequency Control Trans., 49(4), 495-500 (2002).
71. Cagatay, S., B. Koc and K. Uchino, A 1.6 mm Metal Tube Ultrasonic Motor, IEEE Trans.- UFFC, 50(7), 782-786 (2003).
72. Uchino, K., Piezoelectric Actuators 2004- Materials, Design, Drive/Control, Modeling and Applications, Proc. 9th Int'l Conf. New Actuators, A1.0, p. 38-48, Bremen, Germany, June 14-16 (2004).
73. https://www.samsung.com/us/mobile/phones/all-phones/
74. Mulvihill, M., K. Uchino, G. Knowles, R. Harbaugh, Piezoelectric Micro-Disruptor for Disrupting a Blockage, Provisional Patent Application No. 11/636,929 (September, 2008).
75. Uchino, K. Entrepreneurship for Engineers, CRC Press, NY (2009). ISBN 978-1-4398-0063-8